Proceeding of the IEEE
International Conference on Robotics and Biomimetics
Dali, China, December 2019

# Control of the Two-wheeled Inverted Pendulum (TWIP) Robot Moving on the Continuous Uneven Ground

Haitao Zhou, Xu Li, Haibo Feng, Enbo Li, Pengchao Ding, Yanwu Zhai, Songyuan Zhang, Yili Fu

***Abstract*— Uneven terrain is common in natural environment. The TWIP robot has demonstrated its rapid movement ability in even ground in previous works. This paper explores control of the TWIP robot in the continuous uneven ground except the step case. The sinusoidal function and the piece-wise linear function type ground surface are taken as an example to explore motion characteristics of robots on complex terrain. As for the robotic system, continuous or step changes of slope are the main types of disturbance to it. To cope with these disturbance, a Sliding Mode Control (SMC) is used to design the nominal controller due to its insensitivity to uncertainty. Then, the Extended Kalman Filter (EKF) is adopted to estimate the slope of unknown terrain without any ground information from sensors but according to motion state of robot and the Equilibrium Point Estimation (EPE) is then achieved based on the obtained slope angle. In simulation,the TWIP robot moves on these two types of uneven ground surface to track the reference position or velocity trajectory. The comparative experimental results have demonstrated that SMC combined with the EPE method can enable TWIP robot to locomote on some limited uneven ground with higher stability and dynamic performance, compared to the single LQR and the single SMC method. Also, the proposed algorithm has been conduted successfully on the WIP-Bot robot to travel upward and downward slope.**

## I. INTRODUCTION

Up to now, the existing TWIP robots have been widely applied to implement some specific tasks, such as people tending to ride Segway [1] personal vehicle to travel in a short distance or the manipulation mobile robots [2][3] used to perform operational tasks in place of humans. However, these application are currently only limited to the human environment, where the floors are flat enough to ensure stable motion of robots. However, the TWIP robots moving on irregular ground presents a challenging problem, as they are easy to topple over if no valid control algorithm used to keep its equilibrium.

When the robots move on horizontal ground, we can use simple dynamic model as presented in [4-6] to design the linear or nonlinear controllers. What's more, it does not require much work to handle large uncertainties of system and external disturbances. This situation has changed as the robots locomote in complex terrain. Both the change of ground slope and the unexpected collision between wheel and ground surface will bring large disturbance to the nominal system of robots during the movement process. In general, there is no sensor can be used to detect these ground information beforehand, which much depend on algorithm to keep balance after the collision has occurred.

Research supported by the Foundation for Innovative Research Groups of the National Natural Science Foundation of China (Grant No.51521003).(corresponding author :Yili Fu and Haibo Feng)

Haitao Zhou, Haibo Feng and Yili Fu are with State Key Laboratory of Robotics and System, Harbin Institute of Technology, Harbin, Heilongjiang Province, 150001, China htzhouhit@126.com, haibofeng@hotmail.com, yilifu417@126.com

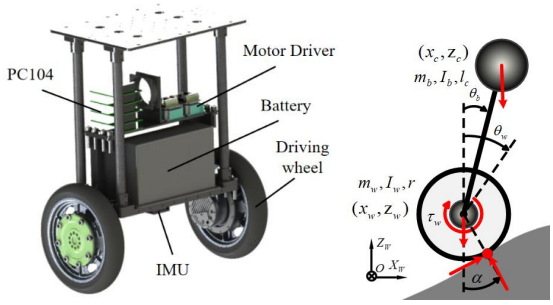


Fig. 1. Left: WIP-Bot robotic platform. Right: Schematics of TWIP robot on a slope.

There are two approaches can be used to enable the two-wheel mobile robots to locomote in complex terrain. The first one is to find a robust control algorithm, which can resist large disturbance. The sliding mode [7] might be an effective method to achieve this goal, as it is less sensitive to uncertainty and disturbance compared to other controllers, such as PID, pole placement and LQR. The sliding mode with specially designed sliding surface in [8] and the integral sliding mode in [9] have separately demonstrated great effectiveness of the accurate position tracking control of the two-wheel mobile robots on the slope. However, their researches are only limited to fixed-angle slopes and the constant value of slope angle is directly used for controller design, which is much different from the case studied in this paper.

The second approach aims to solve this problem by adding additional mechanisms and actuators to the customary system. A type of two-wheel personal mobility robots is developed in [10] to facilitate convenient personal mobility even in outdoor environment and the mechanical structure consists of a seat slider and two independent leg wheels attached on either side. The two-wheel mobile manipulator developed by Stilman in [11][12] is such a system that can use upper body articulation to improve acceleration performance and stability. Takaki in [13] designed a planetary wheel mechanism to enable the inverted pendulum robot to climb stairs with a height of 120 mm-130mm. The two-wheel legged robots [14-17] combining both leg mechanism and two driving wheel are able to adapt to some limited rough terrain, while possessing dynamic stability as the conventional two-wheel

978-1-7281-6321-5/19//$31.00 ©2019 IEEE

mobile robots. However, these enhanced two-wheel mobile robots are complicated in mechanical structure and is much difficult to design.

For some special terrain that human or robots might encounter, such as the steps, it presents more challenging than moving on the slope for the robot. To analyze it, issues related to dynamic behavior on corner point, impact or flight dynamics should be resolved [18][19] but not included in our research. The well-known TWIP robot nBot has demonstrated its ability to move in various outdoor terrain as shown in some corresponding vedios [20]. Unfortunately, the control techique utilized is rarely introduced. Kausar explores the control problem of TWIP robot in uneven terrain, such as a ramp [21][22], which is similar to our research. He derived dynamics fully considering variation of surface of terrain, and then a full state feedback controller combined with gain scheduling is adopted to ensure stability. In contrast, we use a nonlinear control approach SMC rather than the linear control method to design the baseline controller, which can ensure great dynamic performance in a large workspace. Also, the EPE method is proposed to estimate equilibrium point to compensate for the error of robot rather than obtain it directly according to the generated bump function like in [21].

The rest of this paper is organized as follows. Section II presents both the dynamic modelling of TWIP robot on uneven ground and mathematical description of these two types of uneven ground. In section III, the SMC combined with EPE method is designed. The simulation of two-wheel mobile robot moving on uneven ground are described in Section IV. Finally, Section V contains conclusion and future works.

TABLE I
CONTROL VARIABLES AND PARAMETERS

| Symbols | Description |
|---|---|
| $\theta_w$ | Rotation angle of the driving wheel (in radians) |
| $\theta_b$ | Tilt angle of the body (in radians) |
| $\theta_b^*$ | Equilibrium tilt angle (in radians) |
| $r$ | Radius of the driving wheel (in meters) |
| $l_c$ | Distance between the wheel axis and center of mass of the body (in meters) |
| $I_b$ | Moments of inertia of the body with respect to driving wheel axis |
| $\alpha$ | The slope of uneven terrain |
| $c_w$ | Viscous damping coefficient of rotation of the wheel |
| $\tau_w$ | Torque provided by motor of wheel |
| $(x_c, z_c)$ | Coordinates of center of mass of body |
| $(x_w, z_w)$ | Coordinates of center of wheel axis |

## II. MODELING OF ROBOT AND TERRAIN

### A. Dynamic Model

The two-wheel mobile robot systems are modeled as the Two-Wheel Inverted Pendulum (TWIP) when moving on uneven ground in sigittal plane, as shown in Fig. 1. The symbols used as well as their corresponding representations are shown in Table I. The terrain will influence the methemetical model of the TWIP robot [6], as the derived dynamics will include additional terms related to the changes of ground surface compared to the case in flat ground. Accurate detection of terrain variation information is necessary, which is beyond the research scope of this paper. So the dynamic model of robot on the fixed slope is adopted and analyzed.

Also, we only focus on our research in sagittal plane and the tilt or uneven between left and right wheels will be not involved. Select $\mathbf{q_w} = \left[\ \theta_w, \theta_b\ \right]^{\mathrm{T}}$ as the generalized state vector of robot. The Lagrange's method is adopted to analyze the dynamics of this system, which leads to an underactuated model given by

$$\begin{aligned}&(I_b + m_b l_c^2)\ddot{\theta}_b + m_b r l_c \cos(\theta_b + \alpha)\ddot{\theta}_w - m_b g l_c \sin\theta_b \\ &- c_w(\dot{\theta}_w - \dot{\theta}_b) + \tau_w = 0 \end{aligned} \tag{1}$$

$$\begin{aligned}&m_b r l_c \cos(\theta_b + \alpha)\ddot{\theta}_b + (I_w + m_b r^2 + m_w r^2)\ddot{\theta}_w \\ &+ (m_w + m_b) g r \sin\alpha - m_b r l_c \dot{\theta}_b^2 \sin(\theta_b + \alpha) \\ &+ c_w(\dot{\theta}_w - \dot{\theta}_b) - \tau_w = 0 \end{aligned} \tag{2}$$

For further analysis, rearranging the equations of motion of the TWIP model yields

$$\overline{M}\ddot{\theta}_b = \overline{a}_1 + \overline{b}_1 \cdot u \tag{3}$$

$$\overline{M}\ddot{\theta}_w = \overline{a}_2 + \overline{b}_2 \cdot u \tag{4}$$

where parameters $\overline{M}$, $\overline{a}_1$, $\overline{b}_1$, $\overline{a}_2$ and $\overline{b}_2$ satisfy the following equations

$$\overline{M} = m_{11} m_{22} - m_{12}^2 \cos^2(\theta_b + \alpha) \tag{5}$$

$$\begin{aligned}\overline{a}_1 =& n_{12} m_{12} \sin\theta_b - n_{12} m_{12} \sin(\theta_b + \alpha)\cos(\theta_b + \alpha)\dot{\theta}_b^2 \\ &+ n_{22} m_{12} \sin\alpha \cos(\theta_b + \alpha)\end{aligned} \tag{6}$$

$$\overline{b}_1 = - m_{22} - m_{12}\cos(\theta_b + \alpha) \tag{7}$$

$$\begin{aligned}\overline{a}_2 =& - n_{12} m_{12} \cos(\theta_b + \alpha)\sin\theta_b + m_{11} m_{12} \sin(\theta_b + \alpha)\dot{\theta}_b^2 \\ &- m_{11} n_{22} \sin\alpha\end{aligned} \tag{8}$$

$$\overline{b}_2 = m_{11} + m_{12}\cos(\theta_b + \alpha) \tag{9}$$

where $m_{11} = I_b + m_b l_c^2$, $m_{12} = m_{21} = m_b r l_c$, $m_{22} = I_w + m_b r^2 + m_w r^2$, $n_{12} = m_b g l_c$ and $n_{22} = (m_w + m_b) g r$. Also, non-slip condition is assumed throughout the analysis. Note that due to the reason that knowledge of the slope angle is unknown to the robot without information from sensors, the dynamic model considered is a nominal system with parameter uncertainties, which is caused by varied $\alpha$. When moving on horizontal ground, the equilibrium point of two-wheel mobile robot changes with the variation of the slope

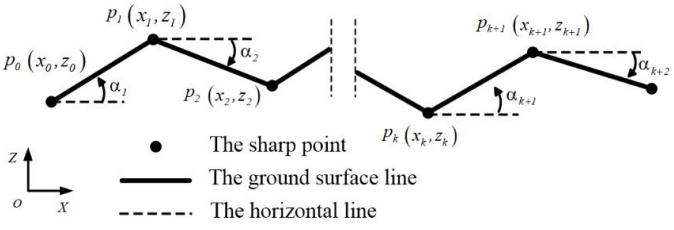


Fig. 2. The piece-wise linear terrain surface.

angle. Combining eq. (1) and eq. (2), and assuming $\ddot{\theta}_b$, $\dot{\theta}_b$, $\ddot{\theta}_w$, $\dot{\theta}_w$ to be zero, the equilibrium state $[\theta_b^*, \dot{\theta}_b^*, \dot{\theta}_w^*]$ of robot satisfy

$$\begin{aligned} \dot{\theta}_b^* = 0, \dot{\theta}_w^* = constant \\ m_b g l_c \sin\theta_b^* = (m_w + m_b) g r \sin\alpha \end{aligned} \tag{10}$$

where the desired tilt angle of body in equilibrium state $\theta_b^*$ is only dependent on the slope angle of ground with the ground resistence neglected. Note that in real control and its implementation on the robot, the estimation $\hat{\theta}_b^*$ is adopted in controller design as we can't obtain its real value $\theta_b^*$ accurately.

### B. Uneven Terrain Description

The uneven ground is represented by the four dimensional vector as $p = [x, z, \alpha, \gamma]^{\mathrm{T}} \in \mathbb{R}^4$, where $x$, $y$, $\alpha$, $\gamma$ are the current wheel ground contact point coordinate, the slope and the curvature of current contact region, respectively. Assume that $\Theta$ is all the possible ground surface space in sagittal plane, which are a set of functions of position $x$. For simplicity, we focus our attention on these types of ground surfaces in this paper, which can be described by the sinusoidal and the piece-wise linear function, included in $Z_s$ and $Z_l$ function spaces, respectively. The mathematical description of the terrain models will be presented as follows.

- The Sinusoidal Function

The sinusoidal functions consists of a series of uniformly convergent triangular functions. Define the parameter vector of the sinusoidal function as $p_{sk}$=$[A_k$,$l_{ck}$,$\lambda_{ck}$,$B_k$,$l_{sk}$,$\lambda_{sk}]^{\mathrm{T}}$, which are the magnitude, frequency and phase of the $k$-th order trigonometric function terms. Assume, $p_{sk} \in \chi_{sk} = \left\{ p_{sk} \in \mathbb{R}^6 \middle| \underline{p}_{sk} \le p_{sk} \le \overline{p}_{sk}, \underline{p}_{sk}, \overline{p}_{sk} \in \mathbb{R}^6, k \in Q \right\}$. Hence, the set of the whole parameters can be included in $\chi_s = \chi_{s1} \cup \chi_{s2} \cup \chi_{s3}, \cdots, \chi_{sn}$. Then, based on $\chi_s$ the set of sinusoidal functions are $Z_s = \{ z_s(x) | z_s(x) = A_0/2 + \sum_{k=1}^{\infty} [A_k \cos(2\pi x/l_{ck} + \lambda_{ck}) + B_k \sin(2\pi x/l_{sk} + \lambda_{sk})], p_{sk} \in \chi_s, k \in Q \}$ and satisfy $Z_s \subset \Theta$. The evolution of the terrain function with respect to the displacement $x$ and the tilt angle of the smooth ground can be separately derived as

$$\dot{z}_s = \frac{d(z_s)}{dx}, \alpha(x) = \arctan(\dot{z}_s) \tag{11}$$

To guarantee there is only one single contact point between the wheel and ground, the curvature of the generated continuous function at every point must be larger than the radius of wheel. In addition, the slope should be bounded in some limits. Hence, the generated functions must satisfy the constraints set as

$$Z_s \subset \Theta_s = \left\{ z_s \middle| |\arctan(\dot{z}_s)| \le \alpha_{max}, \frac{[1 + \dot{z}_s^2]^{\frac{3}{2}}}{|\ddot{z}_s|} \ge r \right\} \tag{12}$$

The sinusoidal function is featured as: (1) The ground surface is continuous, when $x \in [\underline{x}, \overline{x}]$. (2) The slope of ground changes continuously, when $x \in [\underline{x}, \overline{x}]$.

- The Piece-wise Linear Function

The piece-wise linear function consists of a series of linear segments with different slope and length. The corresponding parameter vector of the $k$-th linear function is selected as $p_{lk} = [x_k, z_k, \alpha_k]^{\mathrm{T}}$ and satisfies $p_{lk} \in \chi_{lk} = \left\{ p_{lk} \in \mathbb{R}^3 \middle| \underline{p}_{lk} \le p_{lk} \le \overline{p}_{lk}, \underline{p}_{lk}, \overline{p}_{lk} \in \mathbb{R}^3, k \in Q \right\}$. Then, the whole parameter set is computed as $\chi_l = \chi_{l1} \cup \chi_{l2} \cup \chi_{l3}, \cdots, \chi_{ln}$. So, the set of piecewise linear segments function is formed as $Z_l = \{ z_l(x) | z_l(x) = \tan\alpha_k \cdot (x - x_{k-1}) + z_{k-1} \quad, x \in [x_{k-1}, x_k], p_{lk} \in \chi_l, k = 1, 2, 3, \cdots, n \}$, where $x_0, x_1, x_2 \cdots$ are the sharp points, as shown in Fig. 2. Considering that the slope angle is limited in a range, the following constraint should satisfy

$$Z_l \subset \Theta_l = \{ z_l : |\alpha_k| \le \alpha_{max}, k \in Q \} \tag{13}$$

The sinusoidal function is featured as: (1) The ground surface is continuous, when $x \in [\underline{x}, \overline{x}]$. (2) The slope of ground changes abruptly with a jump at the sharp points when $x = x_0, x_1, x_2, \cdots, x_n$, which will cause a large disturbance to the robot.

## III. CONTROL ARCHITECTURE

### A. Sliding Mode Controller

Choose the state vector as $\mathbf{x} = \left[ x_1, x_2, x_3, x_4 \right]^{\mathrm{T}} = \left[ \theta_b, \dot{\theta}_b, \theta_w, \dot{\theta}_w \right]^{\mathrm{T}} \in \mathbb{R}^4$ and the state space equation can be written as

$$\dot{\mathbf{x}} = \mathbf{f}(\mathbf{x}, \alpha) + \mathbf{g}(\mathbf{x}, \alpha) \cdot u \tag{14}$$

where the nonlinear vectors $\mathbf{f}(\mathbf{x}, \alpha)$ and $\mathbf{g}(\mathbf{x}, \alpha)$ can be expressed as

$$\begin{aligned} \mathbf{f}(\mathbf{x}, \alpha) &= \left[ x_2, f_1(\mathbf{x}, \alpha), x_4, f_2(\mathbf{x}, \alpha) \right]^{\mathrm{T}} \in \mathbb{R}^4 \\ \mathbf{g}(\mathbf{x}, \alpha) &= \left[ 0, g_1(\mathbf{x}, \alpha), 0, g_2(\mathbf{x}, \alpha) \right]^{\mathrm{T}} \in \mathbb{R}^4 \end{aligned} \tag{15}$$

where $f_1(\mathbf{x}, \alpha) = \overline{a}_1/\overline{M}$, $g_1(\mathbf{x}, \alpha) = \overline{b}_1/\overline{M}$, $f_2(\mathbf{x}, \alpha) = \overline{a}_2/\overline{M}$, $g_2(\mathbf{x}, \alpha) = \overline{b}_2/\overline{M}$. Due to the reason that the slope angle of terrain can't be measured directly by the robot, we are unable to obtain the real value of it and parameter uncertainties exist in the dynamic system. In traditional SMC controller design, these uncertainties with respect to varied slope angles are restricted in a specified limitation, instead of estimating it by means of disturbance observers or the dynamic principle. So we rewrite eq. (14) as

$$\dot{\mathbf{x}} = \hat{\mathbf{f}}(\mathbf{x}) + \mathbf{\Delta f}(\mathbf{x}, \alpha) + [\hat{\mathbf{g}}(\mathbf{x}) + \mathbf{\Delta g}(\mathbf{x}, \alpha)] \cdot u \tag{16}$$

where model uncertainty terms can be expressed as $\mathbf{\Delta f}(\mathbf{x}, \alpha) = \mathbf{f}(\mathbf{x}, \alpha) - \hat{\mathbf{f}}(\mathbf{x})$, $\mathbf{\Delta g}(\mathbf{x}, \alpha) = \mathbf{g}(\mathbf{x}, \alpha) - \hat{\mathbf{g}}(\mathbf{x})$. To be further, uncertainty vectors are $\mathbf{\Delta f}(\mathbf{x}, \alpha) = \left[ 0, \Delta f_1(\mathbf{x}, \alpha), 0, \Delta f_2(\mathbf{x}, \alpha) \right]^{\mathrm{T}} \in \mathbb{R}^4$ and $\mathbf{\Delta g}(\mathbf{x}, \alpha) = \left[ 0, \Delta g_1(\mathbf{x}, \alpha), 0, \Delta g_2(\mathbf{x}, \alpha) \right]^{\mathrm{T}} \in \mathbb{R}^4$. The generated uneven terrain must meet the traverse condition of the two-wheel mobile robots, where the slope angle is limited in $[-\alpha_{max}, +\alpha_{max}]$. Also, the model parameter uncertainties are all bounded. Hence, we derived that the the lumped model uncertainties are bounded by the following equations as $|\Delta f_1(\mathbf{x}, \alpha)| \le \rho_{f_1}$, $|\Delta f_2(\mathbf{x}, \alpha)| \le \rho_{f_2}$,

$|\Delta g_1(\mathbf{x},\alpha)| \le \rho_{g_1}$, $|\Delta g_2(\mathbf{x},\alpha)| \le \rho_{g_2}$. Note that $\rho_{f_1}$, $\rho_{f_2}$, $\rho_{g_1}$ and $\rho_{g_2}$ are positive constants, which can be determined once the uneven terrain has been generated or the robotic system has been specified.

In order to control both the movement velocity and displacement of the TWIP robots, the sliding mode surface is selected as

$$s = \mathbf{c} \cdot \tilde{\mathbf{x}} \tag{17}$$

where the coefficient vector is $\mathbf{c} = \begin{bmatrix} c_1, c_2, c_3, 1 \end{bmatrix}$; the tracking error vector is expressed as $\tilde{\mathbf{x}} = \mathbf{x} - \mathbf{x^r}$, which is deviation relative to the desired state vector $\mathbf{x^r} = \begin{bmatrix} \theta_b^{ref}(t), 0, \int \dot{\theta}_w^{ref}(t)dt, \dot{\theta}_w^{ref}(t) \end{bmatrix}^{\mathrm{T}}$. In general, we use $\theta_b^r(t) = \theta_b^*(t)$ to provide a accuracy reference for the dynamic system.

The SMC control law is derived from the equation $\dot{s} = c \cdot \dot{\tilde{x}} = 0$, which can be further written in standard form as

$$\begin{aligned} u =& -[\mathbf{c} \cdot \hat{\mathbf{g}}(\mathbf{x})]^{-1}[\mathbf{c} \cdot \hat{\mathbf{f}}(\mathbf{x}) + \rho \cdot sgn(s)] \\ =& -(\hat{g}_1 c_2 + \hat{g}_2)^{-1}[c_1 x_2 + c_2 \hat{f}_1 + c_3 x_4 + \hat{f}_2 + \rho \cdot sgn(s)] \end{aligned} \tag{18}$$

Define two different nonlinear functions with respect to dynamic uncertainty as

$$f_{\Delta f} = \frac{(\mathbf{c}\hat{\mathbf{g}}) \cdot (\mathbf{c}\boldsymbol{\Delta}\mathbf{f})}{\mathbf{cg}}, f_{\Delta g} = \frac{(\mathbf{c}\hat{\mathbf{f}}) \cdot (\mathbf{c}\boldsymbol{\Delta}\mathbf{g})}{\mathbf{cg}} \tag{19}$$

As each term in nonlinear function is bounded by a specific limits, we obtained $|f_{\Delta f}| \le \rho_f$, $|f_{\Delta g}| \le \rho_g$. The switching gain is designed as

$$\rho = \rho_0 + \rho_f + \rho_g \tag{20}$$

where $\rho_f$ and $\rho_g$ are the upper bound of the nonlinear function $f_{\Delta f}$ and $f_{\Delta g}$, respectively. Then, $\rho_0$ is a positive constant.

Proof: Choose the non-negative quadratic function as $V = s^2/2$. Take the derivative of $V$ with respective time and we get

$$\begin{aligned} \dot{V} =& s\dot{s} \\ =& s\mathbf{c}\left\{\hat{\mathbf{f}} + \boldsymbol{\Delta}\mathbf{f} + (\hat{\mathbf{g}} + \boldsymbol{\Delta}\mathbf{g})u\right\} \\ =& s\frac{\mathbf{cg}}{\mathbf{c}\hat{\mathbf{g}}}\left\{\frac{(\mathbf{c}\hat{\mathbf{g}}) \cdot (\mathbf{c}\boldsymbol{\Delta}\mathbf{f})}{\mathbf{cg}} - \frac{(\mathbf{c}\hat{\mathbf{f}}) \cdot (\mathbf{c}\boldsymbol{\Delta}\mathbf{g})}{\mathbf{cg}} - \rho \cdot sgn(s)\right\} \\ \le& \left|s\frac{\mathbf{cg}}{\mathbf{c}\hat{\mathbf{g}}}\right|\left\{\left|\frac{(\mathbf{c}\hat{\mathbf{g}}) \cdot (\mathbf{c}\boldsymbol{\Delta}\mathbf{f})}{\mathbf{cg}}\right| + \left|\frac{(\mathbf{c}\hat{\mathbf{f}}) \cdot (\mathbf{c}\boldsymbol{\Delta}\mathbf{g})}{\mathbf{cg}}\right| - |\rho \cdot sgn(s)|\right\} \\ \le& -\rho_0\left|s\frac{\mathbf{cg}}{\mathbf{c}\hat{\mathbf{g}}}\right| < 0 \end{aligned} \tag{21}$$

Hence, we conclude that the SMC controller designed in this paper can guarantee the asymptotic tracking of the reference velocity or position trajectory.

### B. Equilibrium Point Estimation

Due to the fact that no exterbal sensors are installed on the robot to detect the ground surface information, we adopt the Extended Kalman Filter (EKF) combined with dynamics of robot to estimate the unknown slope. The estimated slope angle is used to compensate for the uncertainty and error of dynamic model and compute the equilibrium point of robot, which are important to reduce the tracking error and improve dynamic performance.

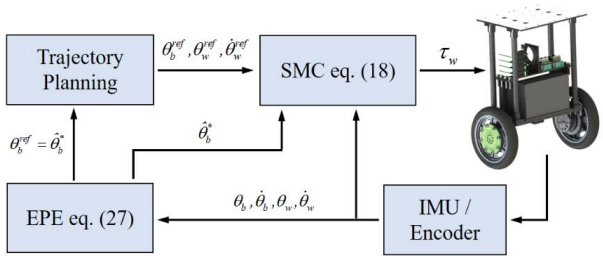


Fig. 3. The control architecture of the TWIP robot.

The EKF is a type of minimum-variance state estimator for nonlinear dynamic systems with Gaussian noise. Choose angle of slope $\alpha$ as the state and the system model is expressed as

$$\begin{aligned} \alpha_{k+1} &= f_k(\alpha_k, w_k) \\ \tau_{wk} &= h_k(\alpha_k, v_k) \end{aligned} \tag{22}$$

where $k$ is the current time step; $\alpha_k$ is the slope angle, state of system when in current contact point; $\tau_{wk}$ is the measurement of motor torque; $w_k$ and $v_k$ are the zero-mean process noise and measurement noise with covariances $Q$ and $R$; $f_k$ and $h_k$ are the nonlinear state and observer function, respectively. Rewriting Dynamic model in eq (2), the nonlinear state function is obtained as

$$\begin{aligned} f_k = \arcsin\Big\{ & n_{22}^{-1}[-m_{12}\cos(\theta_b + \alpha_k)\ddot{\theta}_b - m_{22}\ddot{\theta}_w \\ & + m_{12}\dot{\theta}_b^2 \sin(\theta_b + \alpha_k) - c_w(\dot{\theta}_w - \dot{\theta}_b) + \tau_w]\Big\} \end{aligned} \tag{23}$$

Based on eq (1), the nonlinear observer function is derived as

$$\begin{aligned} h_k =& -m_{11}\ddot{\theta}_b - m_{12}\cos(\theta_b + \alpha)\ddot{\theta}_w \\ & + n_{12}\sin\theta_b + c_w(\dot{\theta}_w - \dot{\theta}_b) \end{aligned} \tag{24}$$

The nonlinear function is expanded into Taylor series and the second order as well as above terms are omitted to obtain an approximate linearized model, which can be expressed as

$$\Phi(k+1) = \frac{d[f(\alpha)]}{d\alpha}, H(k+1) = \frac{d[h(\alpha)]}{d\alpha} \tag{25}$$

The Kalman gain and the optimal estimation of slope are seperately computed as

$$\begin{aligned} K =& \frac{P(k|k-1)H^T}{HP(k|k-1)H^T + R} \\ \alpha(k|k) =& \alpha(k|k-1) + K(\tau_w(k) - H\alpha(k|k-1)) \end{aligned} \tag{26}$$

where $P$ is the covariance corresponding to $\alpha(k|k-1)$. Based on the obtained optimal estimation $\hat{\alpha}$, the equilibrium point is calculated as

$$\hat{\theta}_b^*(t) = \arcsin \frac{(m_w + m_b) r \sin \hat{\alpha}(t)}{m_b l_c} \tag{27}$$

### C. Control Architecture

The control architecture for the TWIP robot is shown in Fig. 3, which include the trajectory planning module, the equilibrium point estimation module, the sliding mode control module and the sensor module. Note that, the estimated equilibrium point is used to compute the reference tilt angle, that is the equilibrium point. Also, based on the estimated slope angle of robot, the model parameter uncertainties can be reduced to some extent, as the dynamics of robot contains several terms related to slope angle of contact ground surface. The sensor module consists of two sensors, the Inertia Measurement Unit (IMU) and wheel encoder, which are used to measure the posture of robot and the wheel velocity or position, respectively. As for the trajectory planning module, a planned veolicty or position trajectory is given in advance. In addition, the robot can receive the velocity commands from remotor manipulated by the operator .

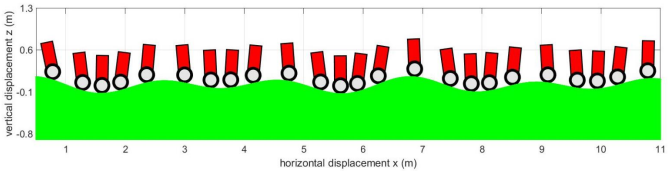


Fig. 4. TWIP robot moves on the Sinusoidal Ground in Matlab simulation.

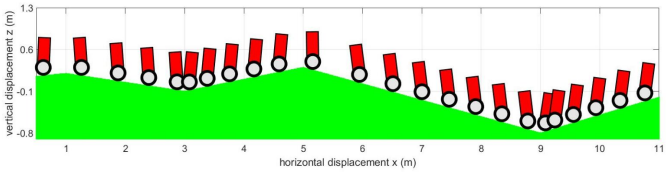


Fig. 5. TWIP robot moves on the Piece-wise Linear Ground in Matlab simulation.

## IV. SIMULATION

The dynamic model parameters of two-wheel robot in this paper are $m_w = 6.62\,kg$, $m_b = 26.293\,kg$, $I_b = 3.004\,kg\,m^2$, $I_w = 0.0189\,kg\,m^2$, $r = 0.107\,m$, $l_c = 0.2953\,m$, $m_b = 26.293\,kg$. Use these parameters to further compute the following constant as $m_{11} = 5.2968\,kg\,m^2$, $m_{12} = m_{21} = 0.8308\,kg\,m^2$, $m_{22} = 0.3957\,kg\,m^2$, $n_{11} = 76.0904\,kg\,m^3/s$, $n_{22} = 34.5126\,kg\,m^3/s$. For comparative analysis, LQR , SMC and SMC combined with EPE method are seperately adopted to design controllers based on dynamics of robots in the following simulation. The coefficients are selected as $c_1 = 15$, $c_2 = 6$, $c_3 = 0.5$ according to the experimental results. More importantly, we set $\rho_{smc} = 10$ in the SMC method only, while $\rho_{epe} = 5$ is selected in SMC coupled with EPE to guarantee the same performance.

LQR approach is designed to minimize the performance index as

$$J = \int_0^\infty [x^T Q x + u^T R u] dt \tag{28}$$

where $Q = [5\ 0\ 0\ 0; 0\ 0\ 0\ 0; 0\ 0\ 300\ 0; 0\ 0\ 0\ 0;]$, $R = 10$ are the weight matrices.

$$u_{lqr} = -K \cdot (x - x^r) \tag{29}$$

where the feedback gain is chose as $K = \left[\, 156.0362, 41.2479, 5.4772, 4.8185 \,\right]^T$; $u_{lqr}$ is the control input obtained from LQR approach. We conducted experiments for two types of uneven ground. Then, the dynamic performance as well as tracking errors is comparatively analyzed to verify the proposed approach.

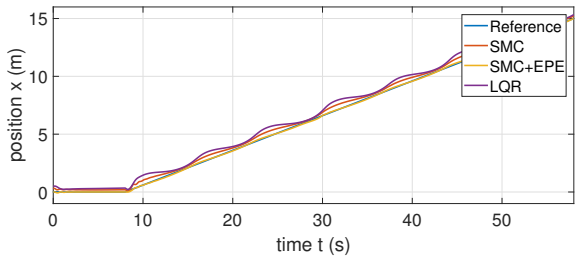


Fig. 6. Position tracking result in the sinusoidal ground case.

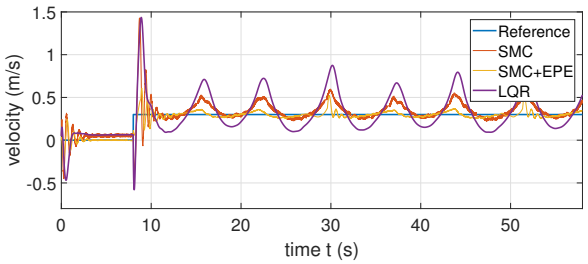


Fig. 7. Velocity tracking result in the sinusoidal ground case.

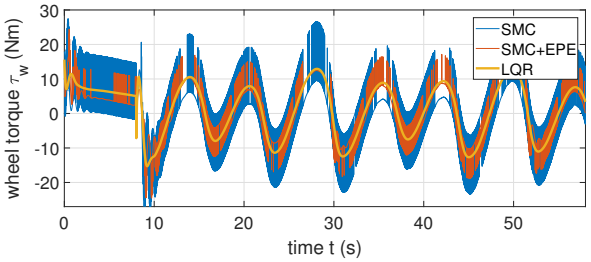


Fig. 8. Control input in the sinusoidal ground case.

### A. Moving on the Sinusoidal Ground Surface

For simplicity, we only consider two triangular terms of the sinusoidal ground surface. The parameters are set as $A_1 = 0.1m$, $A_2 = 0.2m$, $l_1 = 2.1m$, $l_2 = 3.3m$, $\lambda_1 = 0.2m$, $\lambda_2 = 0.9m$. The robot is placed at $x = 0$ point with initial tilt angle set to $0.2rad$, then move with a constant velocity $0.3m/s$ along the uneven ground. The simulation of robot moving on the sinusoidal ground surface is shown in Fig. (4). As shown in Fig. (6) and Fig. (7), the sinusoidal ground surface will significantly affect robot movement state. As the tracking error changes with variation of the sinusoidal

ground accordingly. In addition, the SMC with EPE method have the least tracking error of both position and velocity control compared to SMC and LQR method.

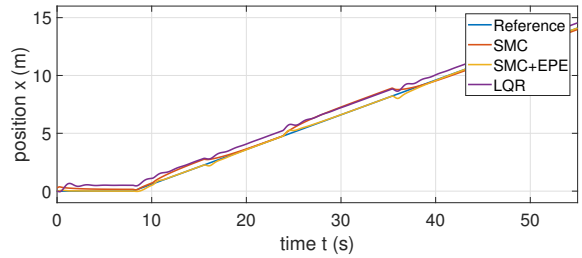


Fig. 9. Position tracking result in the piece-wise linear ground case.

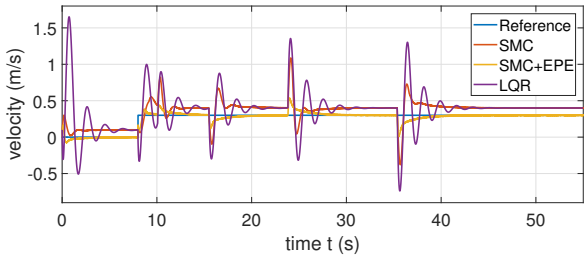


Fig. 10. Velocity tracking result in the piecewise linear ground case.

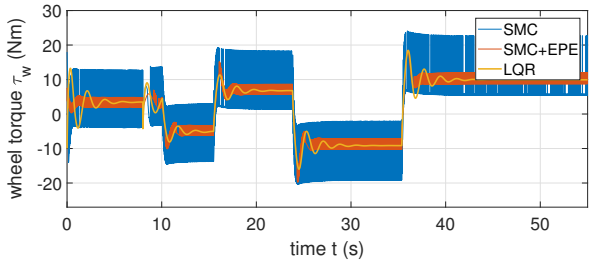


Fig. 11. Control input in the piece-wise linear ground case.

### B. Moving on the Piece-wise Linear Ground Surface

The pirce-wise linear ground is established by setting these sharp points as $p_0 = (-1, 0)$, $p_1 = (1, 0.2)$, $p_2 = (3, -0.1)$, $p_3 = (5, 0.3)$, $p_4 = (9, -0.8)$, $p_5 = (15, 1)$. Then, the tilt angle is computed as $\alpha_1 = 5.71°$, $\alpha_2 = -8.53°$, $\alpha_3 = 11.30°$, $\alpha_4 = -15.38°$, $\alpha_5 = 16.70°$ in each linear slope. The simulation of movement of robot is shown in Fig. (5). When robot moves on the sharp point, there will be a step parameter changes of the dynamic model. Especially, when in concave sharp point case $p_2$ and $p_4$ point, the collision occurred and the velocity changes subsequently. From Fig. (9) and Fig. (10), we can see that the largest disturbance occur at point $p_4$ because of the largest slope changes up to $32.08°$. The EKF is used to estimate slope of ground, but there will be a delay after the changes have happened. Therefore, at every sharp point there will be a position and velocity disturbance to the robotic system. As SMC is less sensitive to uncertainty compared to LQR method, it realizes better tracking performance and recover to the reference velocity and position rapidly after the sharp point. However, the estimated slope used in controller design can further reduce the uncertainty of system and a high robustness to the sharp point disturbance from ground is realized as shown in Fig. (9) and Fig. (10). More importantly, the control input computed from the single SMC method required a large switching length to guarantee its resistance to large uncertainty compared to SMC +EPE method, as shown in Fig. (11).

## V. EXPERIMENT

### A. Robotic Platform Introduction

WIP-Bot robot is developed to demonstrate various advanced control algorithm. The mechanical structure are designed using both 7075 aluminium alloy and carbon fiber, which can ensure the robot to resist large impact when moving on uneven ground.The brushless wheel motors as well as RV reducer can provide control torque up to 19 Nm, which can give enough control torque for the robot to keep balance. The Inertia Measurement Unit (IMU) sensor is located at the bottom of the intermediate body to measure pitch velocity and angle.

### B. Uphill and Downhill Experiment

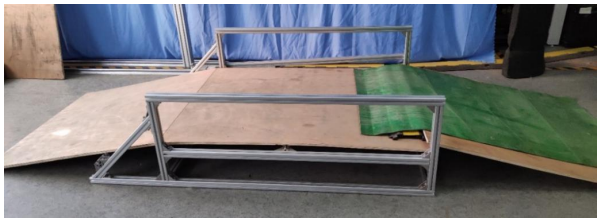

Fig. 12. Experimental environment

The experimental platform is shown in Fig. 12. In experiment, we control the robot to reach an upward slope, then move on a horizontal plat, and finally move through the downward slope to the ground. We give a constant moving velocity of robot. including the upward slope, downward slope and horizontal flat. The snapshots of the WIP-Bot robot in experiment is shown in Fig. 13.

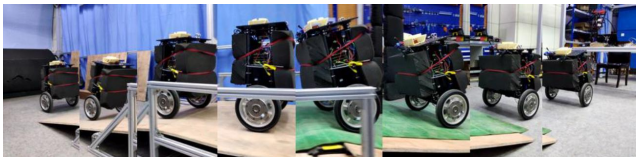

Fig. 13. Snapshots of the WIP-Bot robot traveling the upward and downward slope.

## VI. CONCLUSIONS

This research aims to solve the problem of motion control of the TWIP robot on a relatively simple continuous uneven terrain rather than the step or bump in some literature. Motion control on horizontal ground or slope with fixed angle is mature and various control methods can ensure dynamic performance of robot. However, when the robot moving on some continuous uneven terrain, control approach on horizontal ground can obtain satisfied performance as the varied slope will cause model uncertainty. In addition, the

equilibrium point of robot will change depending on slope of current contact point, which will result in issues of unstability or variation of robot.

To enable the robot successfully to move on uneven ground, this paper proposed a valid control architecture containing various modules. The baseline controller used the SMC method to ensure dynamic performance even far from the equilibrium point. Much importantly, the EKF method combined with dynamics of robot is used to design the EPE estimator to obtain the current slope and compute the equilibrium point. Comparative experiments have demonstrated that SMC + EPE method has achieved great robustness to uncertainty and reduce the tracking errors compared to the single LQR and the single SMC approach. Also, the experiment is conducted on the physical WIP-Bot robot to traveling the upward and downward slope.

In the future, the motion control of TWIP robot in more complicated terrain is expected to be explored, such as steps, bumps, the sharp point contact, which might involve collision with ground and flight in the air of the robot. In addition, the flywheel or swing rod can be attached to the intermediate body of robot, which can be used to provide an extra torque or angular momentum to enhance its stability or dynamic performance on uneven ground.

## ACKNOWLEDGMENT

The authors would like to thank the Heilongjiang Postdoctoral Scientific Research Foundation (LBH-Q17068), the self-managed project of the State Key Laboratory of Robotics and System in Harbin Institute of Technology (SKLRS201801A01, SKLRS201801A02).

## REFERENCES

[1] http://www.segway.com/

[2] Thibodeau, B. J , P. Deegan , and R. Grupen . "Static analysis of contact forces with a mobile manipulator." IEEE International Conference on Robotics Automation IEEE, 2006.

[3] Canete, L. , and T. Takahashi . "Disturbance compensation in pushing, pulling, and lifting for load transporting control of a wheeled inverted pendulum type assistant robot using the Extended State Observer." IEEE/RSJ International Conference on Intelligent Robots Systems IEEE, 2012.

[4] Takei, Toshinobu , R. Imamura , and S. I. Yuta . "Baggage Transportation and Navigation by a Wheeled Inverted Pendulum Mobile Robot." IEEE Transactions on Industrial Electronics 56.10(2009):3985-3994.

[5] Grasser, F . "JOE : A Mobile Inverted Pendulum." IEEE Trans Industrial Electronics 49.1(2002):107-114.

[6] Chan, Ronald Ping Man , K. A. Stol , and C. R. Halkyard . "Review of modelling and control of two-wheeled robots." Annual Reviews in Control 37.1(2013):89-103.

[7] Utkin, V. . "Variable structure systems with sliding modes." IEEE Transactions on Automatic Control 22.2(2003):212-222.

[8] Huang, Jian , et al. "Sliding-Mode Velocity Control of Mobile-Wheeled Inverted-Pendulum Systems." IEEE Transactions on Robotics 26.4(2010):750-758.

[9] Xu, Jian Xin , Z. Q. Guo , and T. H. Lee . "Design and Implementation of Integral Sliding-Mode Control on an Underactuated Two-Wheeled Mobile Robot." IEEE Transactions on Industrial Electronics 61.7(2014):3671-3681.

[10] Tomokuni, N. , and M. Shino . "Wheeled inverted-pendulum-type personal mobility robot with collaborative control of seat slider and leg wheels." IEEE/RSJ International Conference on Intelligent Robots Systems IEEE, 2012.

[11] Stilman, Mike , et al. "Optimized Control Strategies for Wheeled Humanoids and Mobile Manipulators." IEEE-RAS International Conference on Humanoid Robots IEEE, 2009.

[12] Stilman, M , J. Olson , and W. Gloss . "Golem Krang: Dynamically stable humanoid robot for mobile manipulation." IEEE International Conference on Robotics Automation IEEE, 2010.

[13] Takaki, T. , T. Aoyama , and I. Ishii . "Development of inverted pendulum robot capable of climbing stairs using planetary wheel mechanism." IEEE International Conference on Robotics Automation IEEE, 2013.

[14] https://www.bostondynamics.com/handle

[15] https://www.ascento.ethz.ch/

[16] Xu Li, Haitao Zhou, Haibo Feng, Songyuan Zhang, Yili Fu. Design and Experiments of a Novel Hydraulic Wheel-legged Robot (WLR) , IEEE/RSJ International Conference on Intelligent Robots and Systems, 2018.

[17] Haitao Zhou, Xu Li, Haibo Feng, Jiachen Li, Songyuan Zhang, Yili Fu. "Model Decoupling and Control of the Wheeled Humanoid Robot Moving in Sagittal Plane," IEEE/RSJ International Conference on Humanoid Robots, 2019.

[18] Hashimoto. "Development of a stair traversing two wheeled robot." IEEE/RSJ International Conference on Intelligent Robots Systems IEEE, 2012.

[19] Chen, T. , P. Hazelwood , and K. Stol . "Step ascent modelling of a two-wheeled robot." Mechatronics and Machine Vision in Practice (M2VIP), 2012 19th International Conference IEEE, 2012.

[20] http://www.geology.smu.edu/ dpa-www/robo/nbot/

[21] Kausar, Z., Stol, K., Patel, N. (2011). Stability region estimation of statically unstable two wheeled mobile robots. In IEEE International Conference on Robotics and Biomimetics (ROBIO), 2011 (pp. 1379–1384).

[22] Kausar, Z., Stol, K., Patel, N. (2012b). Effect of terrain inclination on performance and stability region of two wheeled mobile robots. IJARS.